LA-UR- 98-2709

Title: On The Transparency of Foam in Low-Density Foam Z-pinch Experiments

CONF-980605--

Author(s):
J. J. MacFarlane
M. S. Derzon
T. J. Nash
G. A Chandler
D. L. Peterson

Submitted to: 12th Topical Conference on High-Temperature Plasma Diagnostics, Princeton, NJ
June 7 - 11, 1998

Los Alamos
NATIONAL LABORATORY

DISCLAIMER

DISCLAIMER

Portions of this document may be illegible in electronic image products. Images are produced from the best available original document.

On The Transparency of Foam in Low-Density Foam Z-pinch Experiments

J. J. MacFarlane

Prism Computational Sciences, Inc., Madison, WI, 53703
and
Fusion Technology Institute, Univ. of Wisconsin, Madison, WI, 53706

M. S. Derzon, T. J. Nash, G. A. Chandler

Sandia National Laboratories, Albuquerque, New Mexico, 87185

D. L. Peterson

Los Alamos National Laboratory, Los Alamos, New Mexico, 87545

Abstract

Foam Z-pinch experiments have been performed on the SATURN and Z machines at Sandia National Laboratories to study physics issues related to x-ray radiation generation and inertial confinement fusion. A significant issue for foam Z-pinch experiments is the transparency of the heated foam as a function of time and wavelength. Foam transparency will be important in future foam Z-pinch experiments both because it influences the time-dependent radiation field seen by an ICF capsule embedded in the foam, and because it is an important factor in making high-resolution spectral measurements of a capsule or tracers embedded in the foam. In this paper, we describe results from simulations and experiments which address the issue of foam transparency. We discuss imaging data from one Z experiment in which x-ray emission from a half-Au/half-CH disk located at the bottom of a 1 cm-tall, 14 mg/cc TPX foam is observed. Simulation results predicting CH foam optical depths as a function of plasma conditions are presented. In addition, we present results from spectral calculations which utilize 2-D MHD simulation predictions for the time-dependent foam conditions. Our results indicate that the observed x-ray framing camera images are consistent with early-time (several ns prior to stagnation) foam electron temperatures of $\gtrsim$ 30 eV, which is somewhat hotter than the foam electron temperatures predicted from the 2-D MHD simulations at early times.

1. Introduction

Z-pinch experiments have been performed on the Z and SATURN pulsed power devices at Sandia National Laboraties over the past several years[1,2,3] to study physics issues related to x-ray radiation generation and inertial confinement fusion (ICF). In Z experiments, currents of approximately 18 MA are obtained in the load, with rise times of $\sim$ 100 ns. In dynamic hohlraum experiments,[1] a tungsten (W) wire array is heated and accelerated radially inward by the magnetic field, striking the outer boundary of a cylindrical foam or foil "target." As the tungsten "stikes" the foam target, a hot radiating plasma is produced as the kinetic (hydrodynamic) energy of the W plasma is converted into internal energy. In some foam experiments, the foam is coated with a thin metal layer (*e.g.*, $\sim 0.2 - 0.5$ μm of Au or Cu) to enhance the production of x-ray radiation generated during the strike phase. The W/foam plasma then continues to implode until stagnation on axis, which produces an additional burst of radiation. In the dynamic hohlraum ICF concept (see Figure 1(a)) an ICF capsule located at the center of the pinch sees the x-ray radiation field generated by during the strike phase. The capsule can then be spherically imploded prior to the arrival of shocks generated by the inward-moving W/foam.

To diagnose the plasma properties of the foam and/or capsule it can be advantageous to perform high-spectral resolution measurements of the foam, capsule dopants, or localized tracer materials placed in the foam or capsule. To record spectra from, say, a doped capsule, it is of course necessary that the foam not be optically thick at the photon energies of dopant line emission. The issue of foam transparency has been addressed recently in Z experiments in which a small CH disk, half of it coated with a thin layer of Au, was placed at the bottom of the foam target (see Figure 1(b)). Because of the much higher reemission (or albedo) of high-Z materials, the Au can exhibit significantly brighter emission than the CH. X-ray framing camera images were obtained from the on-axis diagnostics package located above the pinch. Resolving the "half-moon" emission from the Au portion of the disk demonstrates that the foam is at least partially transparent at wavelengths where the detector response is relatively high.

In this paper, we briefly discuss one of these experiments, along with simulations meant to provide a better understanding of the foam opacity at relatively early times in the x-ray pulse (several ns prior to stagnation). We also describe numerical calculations of the frequency-dependent foam opacity, along with simulations of the Au/CH disk emission utilizing foam properties predicted from 2-D MHD simulations performed at Los Alomos National Laboratory (LANL).

2. Experimental Results

A schematic illustration of the target/wire array geometry for Z shot Z-216 is shown in Figure 1(b). The W wire array consisted of 290 wires of diameter 7.5 μm and total mass of 2.5 mg. The original diameter of the wire array was 4 cm. The foam target was an uncoated 14 mg/cc TPX foam with a height of 1 cm and radius of 0.5 cm. The disk at the bottom of the foam target was a 0.5 cm-diameter, 125 μm-thick CH circular disk, one-half of which was covered with a 2 μm-thick layer of Au. A 3 degree glide plane geometry was utilized in this experiment, so that height confining the inward-moving W plasma near the axis was slightly smaller than at the original wire array position. An on-axis diagnostic package viewed the pinch through a 2 mm diameter aperture at the top of the load. The return current can had 9-fold symmetry for the diagnostic slots. Additional details regarding Z experiments and diagnostics can be found in Nash et al.[4]

Figure 2 shows x-ray framing camera images through Be (left image) and Kimfoil (right image) filters. These images were recorded approximately 6 ns prior to stagnation. Figure 3 shows the time-dependent on-axis bolometer measurement for the same shot. Also shown in Figure 3 are timing marks corresponding to the framing camera images. The images in Figure 2 correspond to time mark "2" in Figure 3 ($t = 2.530$ μs). Note that the contrast between the Au and CH portions of the disk persists up to a period approximately 3 ns prior to stagnation. By this time the *radiation* temperature, based on x-ray diode (XRD) measurements, is estimated to be approximately 130 - 140 eV. The peak radiation temperature at stagnation for this shot was about 190 eV.

Note that the radiation temperatures in the foam can significantly exceed the electron temperatures. This is because it takes a finite period of time to radiatively heat the foam. Also, since the foam ionization state should more closely reflect the electron temperature, the foam can in principal remain relatively cool and weakly ionized even thought the radiation temperatures are much higher. This is important because it is the ionization state which determines the opacity, the therefore whether spectral line emission originating from a point within the foam interior (*e.g.*, a capsule) can penetrate the foam.

3. Simulation and Analysis

Radiation-hydrodynamic simulations of shot Z-216 were performed at LANL using a 2-D MHD code. Figure 4 shows results for the radial dependence of the mean electron and radiation temperature in the foam (top plot) and the mean foam density (bottom plot). Here, the radially-dependent mean is defined as the temperature (or density) averaged over the 1 cm height of the foam. The curves correspond to simulation times of 228, 229, and 230 ns. By comparison, the peak radiation flux at stagnation occurs at a simulation time of 234 ns. Thus, the curves at 228 ns correspond to a time approximately 6 ns prior to peak radiation flux, and therefore correspond approximately to the time mark "2" in Figure 3, as well as the time of the x-ray framing camera images in Figure 2.

Note that at these times, the electron temperatures at the center of the foam (near the axis) are predicted to be significantly lower than the radiation temperatures, which range from $T_R \simeq 100$ eV to 180 eV at the simulation times shown. By comparison, the mean electron temperatures at $t = 228$ ns are predicted to be < 30 eV at radii < 1 mm. At larger radii, the electron temperatures are higher due to the compression of the foam.

Figure 5 shows a series of simulated images which were computed using our multi-dimensional spectral analysis code SPECT3D.[5] These simulations utilize the density and electron temperature profiles predicted from the 2-D MHD calculation at a simulation time of 228 ns. Atomic level populations were computed assuming local thermodynamic equilibrium

(LTE). In the SPECT3D simulations, we inserted an optically thick isothermal layer in the bottom spatial zone of the pinch to represent the Au/CH disk. The emission temperatures of the Au and CH portions of the disk were chosen such that the Au and CH disk regions had albedos of 0.78 and 0.20, respectively. The synthetic images shown in Figure 5 include the x-ray framing camera filter response, and represent an on-axis view looking down through the heated foam to the Au/CH disk. The spatial resolution of the images in Figure 5 is limited by spatial grid resolution (0.01 cm by 0.01 cm) used in the 2-D MHD simulation.

The upper left image in Figure 5 was computed using the unmodified 2-D MHD temperature and density profiles. In this case, the contrast along the Au/CH disk boundary is not seen because the CH foam is optically thick. Thus, the simulated image is not consistent with the framing camera data at these relatively early times. Figure 6 shows the calculated frequency-dependent optical depth for a 1 cm-long, 14 mg/cc CH plasma at electron temperatures ranging between 10 eV and 50 eV. Note that at T $\gtrsim$ 30 eV ,the plasma starts to have an optical depth $\lesssim$ 1 just below the carbon K-shell photoionization edge (h$\nu \approx$ 0.4 keV). However, at T $\lesssim$ 20 eV, the foam is optically thick due to L-shell bound-free absorption.

To gain insight into what foam plasma temperatures are required in order to allow the Au/CH disk to be seen, we artificially adjusted the foam temperatures from the MHD simulations to have a minimum electron temperature. Synthetic images are shown in Figure 5 using a minimum temperature of 20 eV (upper right), 30 eV (lower left), and 40 eV (lower right). Note that the intensity scales are different for each image. The calculations indicate when the foam electron temperatures are $\lesssim$ 20 eV, the Au/CH disk should not be seen. However, for temperatures $\gtrsim$ 30 eV, the framing camera images should be able to see emission from the Au/CH disk. It is also worth noting that the Au emission seen by the detector in this simulation is due to photons with energies < 0.3 keV; *i.e.*, in the relatively low energy portion of the framing camera filter response.

Figure 7 shows results for specific intensities and optical depths computed along a line of sight from the detector to a point on the Au disk near the disk center. The purpose of plots of this type is to show where the emission seen by a detector originates in the plasma, and how it is attenuated (or enhanced) on its way to the detector. The left plot corresponds to the case using the unaltered 2-D MHD output, while the right plot corresponds to the case of using a minimum electron temperature in the foam of 40 eV. The optical depths are integrated values from the top of the foam (left boundary of plot). The Au disk is located 1 cm from the top of the foam, and shows the highest specific intensity. The three curves in each plot correspond to photon energies below (hν = 250 eV) and above (hν = 450 eV and 1 keV) the carbon K-edge. The primary differences between the $T_{min} = 0$ and $T_{min} = 40$ eV results are seen in the hν = 250 eV results (solid curves). In the $T_{min} = 40$ eV simulation, 250 eV photons emitted by the bottom disk ($z = 1.0$ cm) are only modestly attenuated by the intervening foam. This is because the line-of-sight foam optical depth at this photon energy is $\approx$ 0.7.

On the other hand, when using the unmodified MHD results, the cooler foam has an optical depth of $\sim$ 10 at hν = 250 eV (upper left plot). Thus, the specific intensity emitted by the Au disk is seen to decrease very sharply as it is attenuated by the foam (going from right to left in the lower plots). Note also that the total foam optical depths are approximately 200 and 20 at $h\nu = .45$ and 1.0 keV, respectively. Even at 3 keV, the optical depth across the foam is ~ 1 at these relatively cool plasma temperatures.

Our results suggest that the radiation field at early times (several ns prior to stagnation) heats the plasmas more rapidly than is predicted by the 2-D MHD simulations of this experiment. Since the earliest framing camera images are able to resolve the Au/CH disk, our calculations indicate that the foam electron temperatures at this time are $\gtrsim$ 30 eV. Thus, the foam appears to be reasonably transparent to $h\nu \sim 200$ - 400 eV radiation for times ranging from ~ 3 ns prior to stagnation to at least 7 ns prior to stagnation. This should in principle allow for the possibility of doing XUV spectroscopy (below the carbon K-edge) of an embedded capsule at these relatively early times. Obtaining soft x-ray spectra from the capsule region will require that the foam be heated to electron temperatures of $\gtrsim$ 100 eV; *i.e.*, hot enough that the carbon K-shell electrons become ionized. Additional work needs to be done to develop a better understanding of the time-dependent heating of the foam and its ionization state. This clearly is an important issue because it also affects the time- and frequency-dependent radiation field seen by the capsule.

4. Acknowledgements

This work was supported in part by Sandia National Laboratories.

References

1. M. K. Matzen, *Phys. Plasmas* **4**, 1519 (1997).

2. R. B. Spielman, C. Deeney, G. A. Chandler, et al., in Dense Z-Pinches, AIP Conference Proceedings, Vol. 409, p. 101 (1997).

3. T. J. Nash, et al., 4th International Conference on High-Density Z-Pinches, Vancouver, CA (1997).

4. T. J. Nash et al., this proceedings (1998).

5. MacFarlane, J. J., et al., presented at the 24th IEEE International Conference on Plasma Science, San Diego, CA (1997).

5. Figure Captions

Figure 1. Schematic illustration of: (a) a dynamic hohlraum Z-pinch load with an ICF capsule embedded in a low-density foam; and (b) a foam Z-pinch load with a Au/CH disk at the bottom of the foam.

Figure 2. On-axis x-ray framing camera images through Be (left) and Kimfoil (right) filters from Shot Z-216. The bright "half-moon" emission is from the Au half of the Au/CH bottom disk.

Figure 3. Time-dependent on-axis bolometer power from Shot Z-216. Also shown (as integers just above the x-axis) are timing references for the x-ray framing cameras. The images in Figure 2 correspond to the time "2" at $t = 2.530$ μs.

Figure 4. Mean temperatures and densities (averaged over the 1 cm height of the foam) predicted by a 2-D MHD simulation of Shot Z-216. In the top plot, radiation temperatures are represented by the dashed curves, while electron temperatures are represented by the solid curves.

Figure 5. Simulated on-axis x-ray framing camera images for Shot Z-216. The time corresponds to approximately time mark "2" in Figure 3. Without modifying the 2-D MHD foam electron temperatures (upper left image), the Au/CH disk cannot be seen. Requiring the electron temperatures throughout the foam to be at least 30 eV (lower left image) and 40 eV (lower right image) allows the Au half-moon to be clearly seen (top half of each image).

Figure 6. Calculated frequency-dependent optical depths for a 1 cm-long, 14 mg/cc CH foam for temperatures ranging from 10 to 50 eV.

Figure 7. Optical depths (upper plots) and specific intensities (lower plots) calculated along a line-of-sight from an on-axis detector to a gold element near the center of the Au/CH disk. The different curves in each plot correspond to photon energies of 250 eV (solid curves), 450 eV (dotted curves) and 1 keV (dashed curves). Left: using the unmodified 2-D MHD foam temperatures and densities. Right: adjusting the foam temperatures to be ≥ 40 eV.

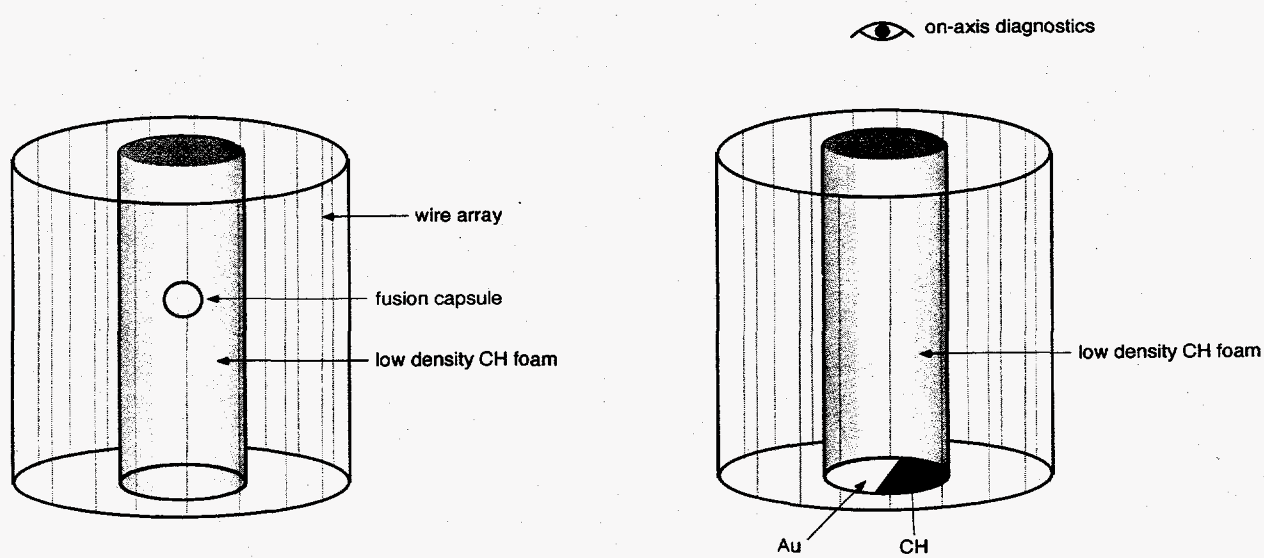

wire array
fusion capsule
low density CH foam
on-axis diagnostics
low density CH foam
Au
CH

(a) (b)

Figure 1.

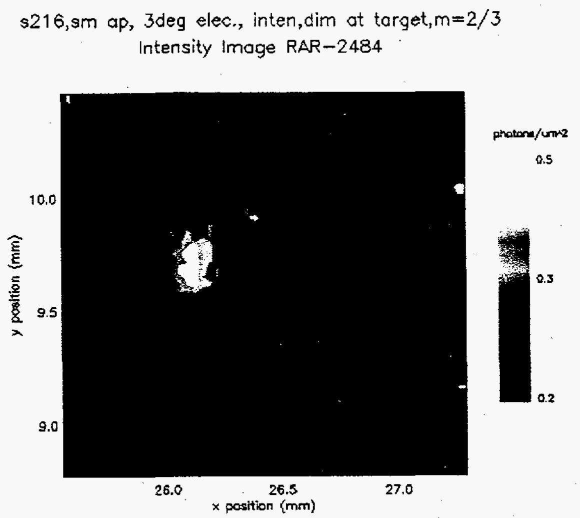

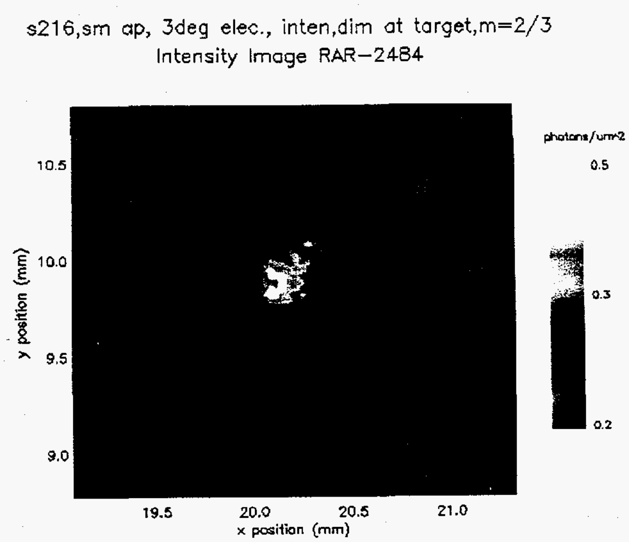

(higher quality color images can be supplied for publication.)

Figure 2.

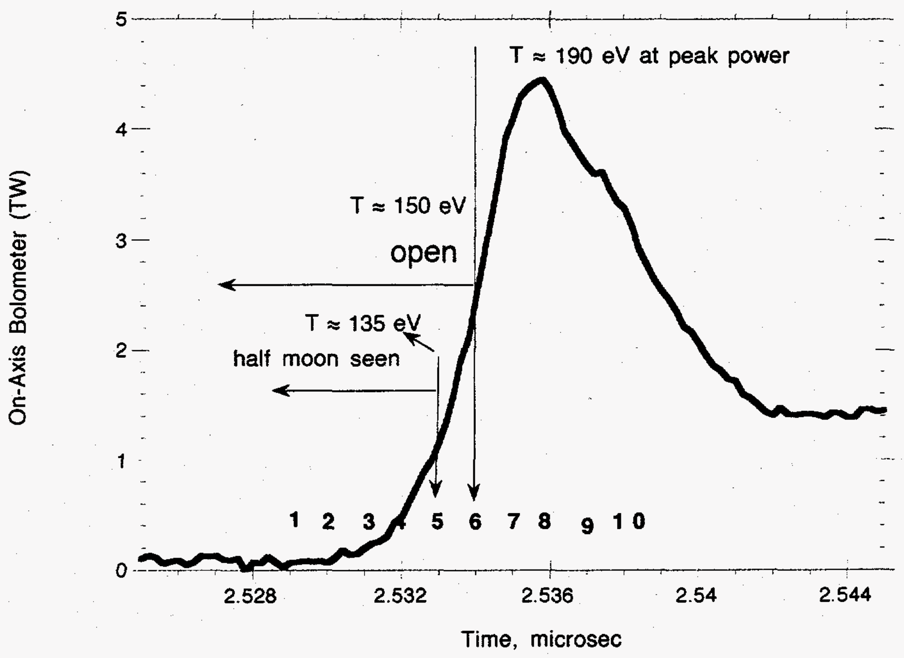
T ≈ 190 eV at peak power
T ≈ 150 eV
open
T ≈ 135 eV
half moon seen
1 2 3 4 5 6 7 8 9 10
On-Axis Bolometer (TW)
0
1
2
3
4
5
2.528
2.532
2.536
2.54
2.544
Time, microsec

Figure 3.

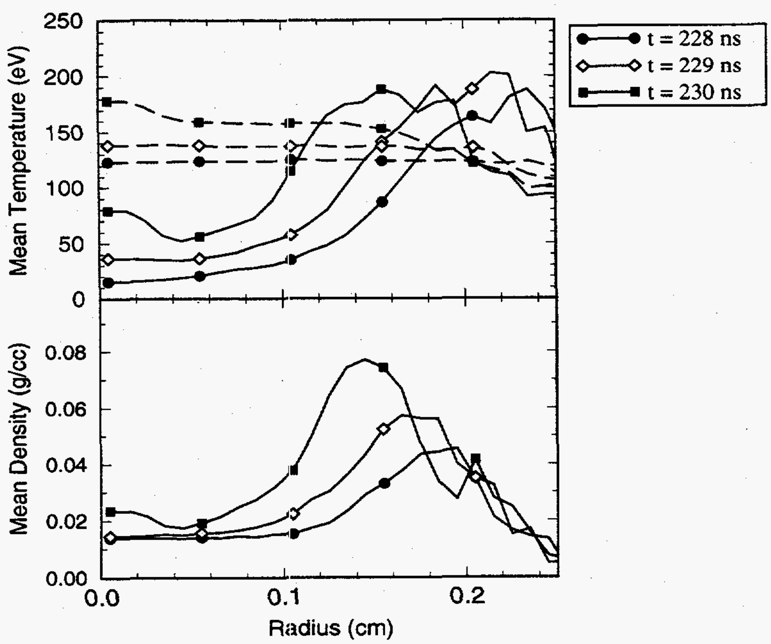

t = 228 ns
t = 229 ns
t = 230 ns
Mean Temperature (eV)
250
200
150
100
50
0
Mean Density (g/cc)
0.08
0.06
0.04
0.02
0.00
0.0
0.1
0.2
Radius (cm)

Figure 4.

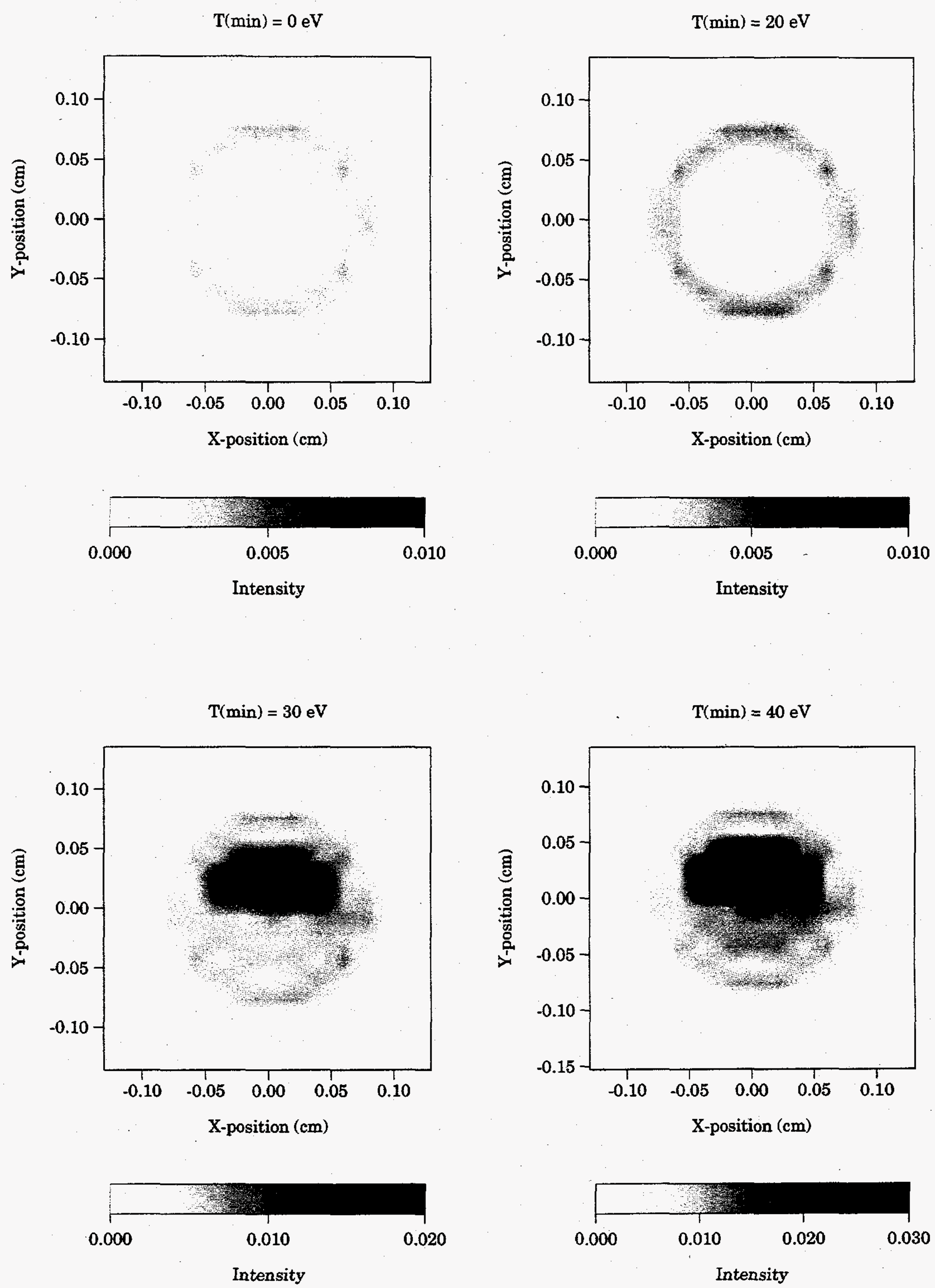
T(min) = 0 eV
T(min) = 20 eV
T(min) = 30 eV
T(min) = 40 eV
Y-position (cm)
X-position (cm)
0.10
0.05
0.00
-0.05
-0.10
-0.15
Intensity
0.000
0.005
0.010
0.020
0.030

Figure 5.

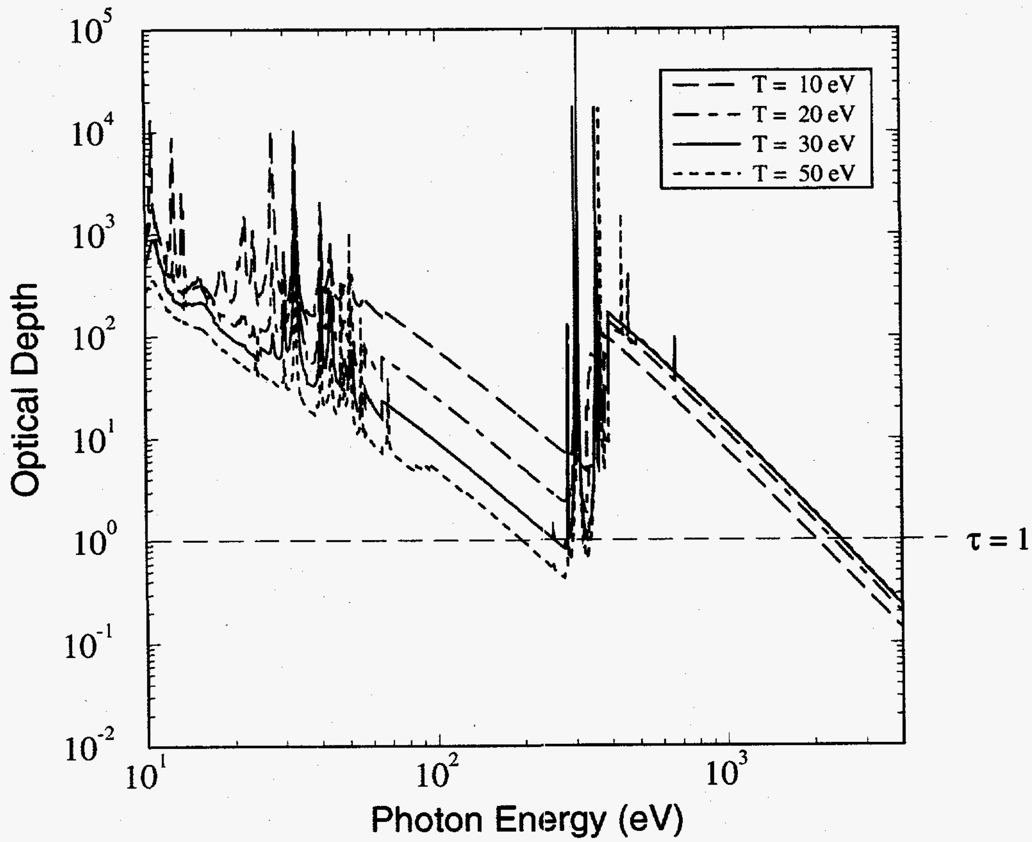
T = 10 eV
T = 20 eV
T = 30 eV
T = 50 eV
τ = 1
Optical Depth
Photon Energy (eV)
10^5
10^4
10^3
10^2
10^1
10^0
10^-1
10^-2
10^1
10^2
10^3

Figure 6.

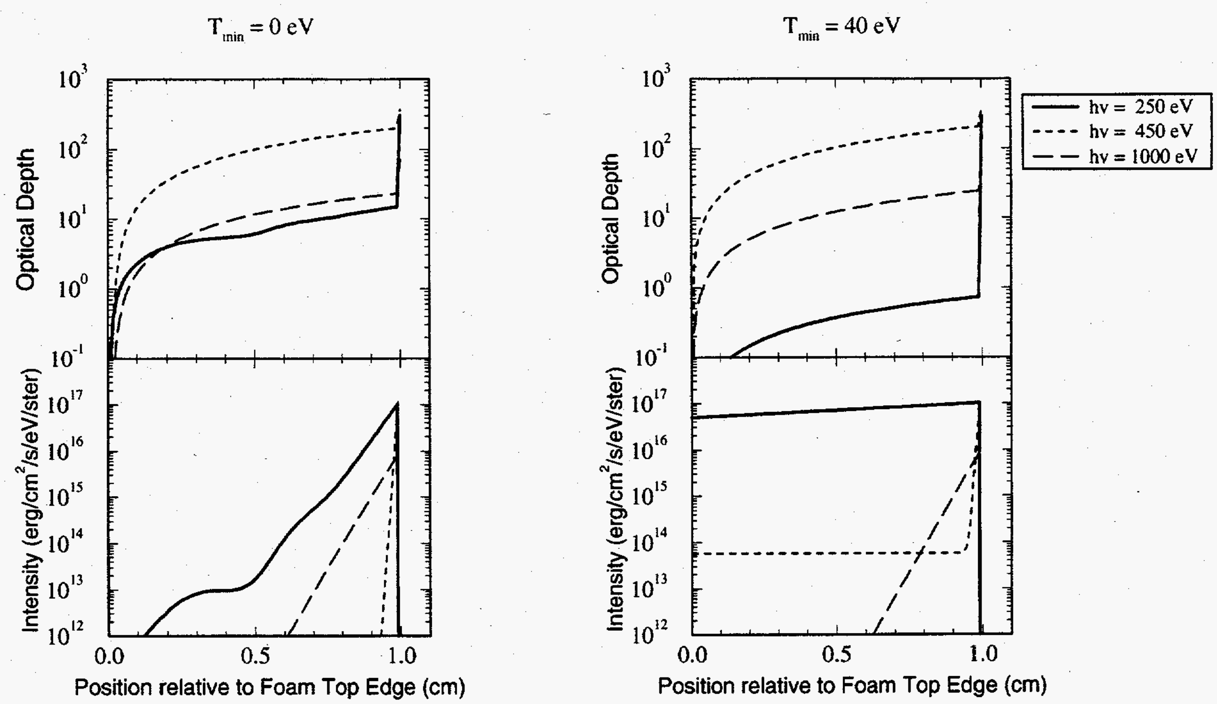
T_min = 0 eV
T_min = 40 eV
Optical Depth
Intensity (erg/cm²/s/eV/ster)
Position relative to Foam Top Edge (cm)
hv = 250 eV
hv = 450 eV
hv = 1000 eV

Figure 7.